Neural Network Application in Asymmetrical 9-Level Inverter

R. Taleb and A. Meroufel

***Abstract*—A neural implementation of an harmonic elimination strategy for the control of a uniform step asymmetrical 9-level inverter is proposed and described in this paper. A Multi-Layer Perceptron (MLP) neural network is used to approximate the mapping between the modulation rate and the required switching angles. After learning, the neural network generates the appropriate switching angles for the inverter. This leads to a low-computational-cost neural controller which is therefore well suited for real-time applications. This neural approach is compared to the well-known Multi-Carrier Pulse-Width Modulation (MCPWM). Simulation results demonstrate the technical advantages of the neural implementation of the harmonic elimination strategy over the conventional method for the control of an uniform step asymmetrical 9-level inverter. The approach is used to supply an asynchronous machine and results show that the neural method ensures a high quality torque by efficiently canceling the harmonics generated by the inverter.**

***Index Terms*—Artificial neural network (ANN), harmonics elimination strategy (HES), multi-carrier pulse-width modulation (MCPWM), multi-layer perceptron (MLP), uniform step asymmetrical multilevel inverter (USAMI).**

I. INTRODUCTION

INVERTERS are widely used in modern power grids; a great focus is therefore made in different research fields in order to develop their performance. Three-level inverters are now conventional apparatus but other topologies have been attempted this last decade for different kinds of applications [1]. Among them, Neutral Point Clamped (NPC) inverters, flying capacitors inverters also called imbricated cells, and series connected cells inverters called cascaded inverters [2]. Of course, these topologies may be combined [3].

This paper is a study about a three-phase multilevel converter based on series connected single phase inverters (partial cells) in each phase. A multilevel converter with k partial inverters connected in serial is presented by Fig. 1. In this configuration, each cell of rank $j = 1, ...k$ is supplied by a dc-voltage source u_{dj}. It has been shown that feeding partial cells with unequal dc-voltages (asymmetric feeding) increases the number of levels of the generated output voltage without any supplemental complexity to the existing topology [4]. These inverters are referred to as "Asymmetrical Multilevel Inverters" or AMI.

Some applications such as active power filtering need inverters with high performances [5]. These performances are obtained if there are still any harmonics at the output voltages and currents. Different Pulse-Width Modulation (PWM) control-techniques have been proposed in order to reduce the residual harmonics at the output and to increase the performances of the inverters [6]. The most popular one is probably the multi-carrier PWM technique [7] which shifts the harmonics to high frequencies by using high-frequency carriers. However, electronic devices and components have limited switching-frequencies. High-frequency carriers are therefore limited by this constraint. An alternative solution consists in adapting the principle of the Harmonics Elimination Strategy (HES) to AMIs. The HES allows canceling the critical harmonic distortions and therefore controlling the fundamental component of the signal by using electronic devices with low switching frequencies.

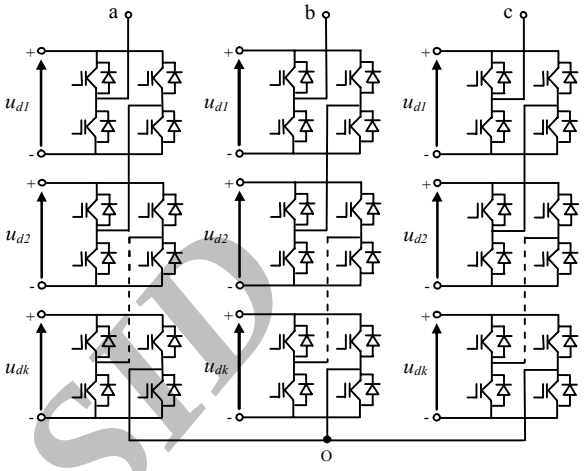

Fig. 1. Three-phase structure of a multilevel converter with k partial monophased inverters series connected per phase.

The principle of this technique relies on the resolution of a system of non linear equations to elaborate the switching angle control signals for the electronic devices [8]. Practically, the implementation of this method requires memorizing all the firing angles which is complex and needs considerable computational costs. Mathematical solutions with limited computational costs are therefore preferably used for real-time applications. The approach can be achieved with Artificial Neural Networks (ANNs) which are known as parsimonious universal approximators. Their learning from examples leads to robust generalization capabilities [9].

This paper proposes a HES based on ANNs to control a 9-level Uniform Step Asymmetrical Multilevel Inverter (USAMI). Standard Multi-Layer Perceptrons (MLP) [10] are used for approximating the relationship between the modulation rate and the inverters switching angles. The performance of this neural approach is evaluated and

Manuscript received May 20, 2009; revised December 1, 2009.

R. Taleb is with the Electrical Engineering Department, Hassiba Ben Bouali University, Hay Es-Salam Chlef, Algeria (e-mail: murad72000@yahoo.fr).

A. Meroufel is with the Intelligent Control and Electrical Power Systems Laboratory (ICEPS), Djillali Liabes University, Sidi Bel-Abbes, Algeria (e-mail: ameroufel@yahoo.fr).

Publisher Item Identifier S 1682-0053(10)1808

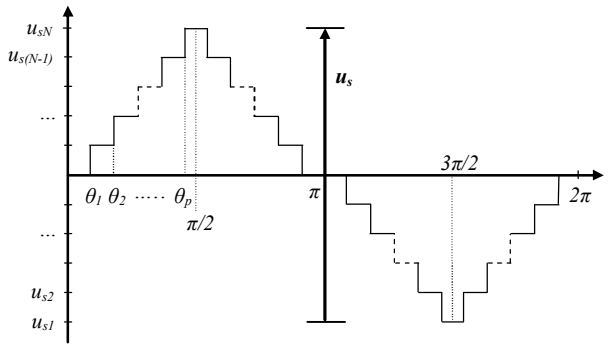

Fig. 2. Typical output voltage waveform of a multilevel inverter.

compared to the MCPWM technique. The proposed neural strategy is also evaluated when the inverter supplies an asynchronous machine. In this application, it is important that the implemented controller computes appropriate switching angles for the inverters in order to minimize the harmonics absorbed by the asynchronous machine. Performances where successfully achieved, the neural controller demonstrates a satisfying behavior and a good robustness.

The paper is organized as follows. USAMIs are described and modeled in Section II. Section III briefly introduces the well-known MCPWM and brings out the original HES based on a MLP. Section IV evaluates the proposed neural strategy in computing optimal angles of an inverter used to supply an asynchronous machine. The results show that the neural method cancels the harmonics distortions and supplies the machine with a well-formed sinusoidal voltage waveform. Conclusions are presented in Section V.

II. UNIFORM STEP ASYMMETRICAL MULTILEVEL INVERTERS

Multilevel inverters generate at the ac-terminal several voltage levels as close as possible to the input signal. Fig. 2 for example illustrates the N voltage levels $u_{s1}, u_{s2}, \ldots u_{sN}$ composing a typical sinusoidal output voltage waveform. The output voltage step is defined by the difference between two consecutive voltages. A multilevel converter has a uniform or regular voltage step, if the steps Δu between all voltage levels are equal. In this case the step is equal to the smallest dc-voltage, u_{d1} [7]. This can be expressed by

$$u_{s2} - u_{s1} = u_{s3} - u_{s2} = \ldots = u_{sN} - u_{s(N-1)} = \Delta u = u_{d1} \qquad (1)$$

If this is not the case, the converter is called a non uniform step AMI or irregular AMI. The control unit defines the switching function s_j of the power switches, and the total *p.u.* output voltage is defined by

$$u_s = \sum_{j=1}^{k} (s_j * u_{dj}) \text{ with } s_j \in \{-1, 0, +1\} \qquad (2)$$

where k represents the number of partial cells per phase. An USAMI is based on dc-voltage sources to supply the partial cells (inverters) composing its topology which respects to the following conditions [7]

$$\begin{cases} u_{d1} \le u_{d2} \le \ldots \le u_{dk} \\ u_{dj} \le 1 + 2\sum_{l=1}^{j-1} u_{dl} \quad (j = 1 \ldots k) \end{cases} \qquad (3)$$

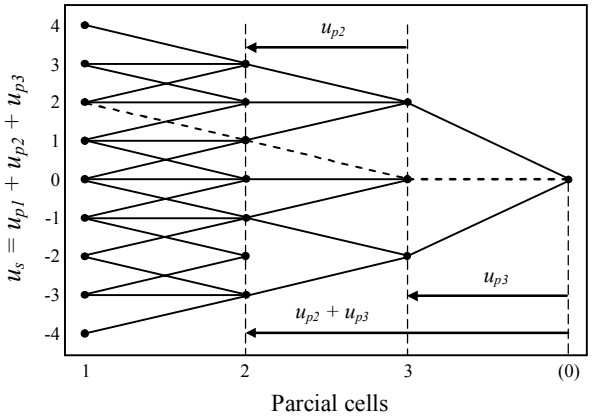

Fig. 3. Possible output voltages of each partial inverter to generate $N = 9$ levels with $k = 3$ cells per phase (with $u_{d1} = 1p.u.$, $u_{d2} = 1p.u.$ and $u_{d3} = 2\,p.u.$).

The number of levels of the output voltage can be deduced from

$$N = 1 + 2\sum_{j=1}^{k} u_{dj} \qquad (4)$$

This relationship fundamentally modifies the number of levels generated by the multilevel topology. Indeed, the value of N depends on the number of cells per phase and the corresponding supplying dc-voltages. Supply partial cells are the complex part in the realization of the inverter and degrade its performances. Different types of supplies, methods of distribution of power and related problems are presented in [4], [11], [12].

Equation (4) accepts different solutions. With k=3 for example, there are two possible combinations of supply voltages for the partial inverters in order to generate a 11-level global output, i.e., $(u_{d1}, u_{d2}, u_{d3}) \in \{(1, 1, 3); (1, 2, 2)\}$, and there are three possible combinations to generate a 15-level global output, i.e., $(u_{d1}, u_{d2}, u_{d3}) \in \{(1, 1, 5); (1, 2, 4); (1, 3, 3)\}$. Fig. 3 shows the possible output voltages of the three partial cells of the 9-level inverter with k=3. The dc-voltages of the three cells are $u_{d1} = 1p.u.$, $u_{d2} = 1p.u.$ and $u_{d3} = 2p.u.$ The output voltages of each partial inverter are noted u_{p1}, u_{p2} and u_{p3} and can take three different values: $u_{p1} \in \{1, 0, 1\}$, $u_{p2} \in \{-1, 0, 1\}$ and $u_{p3} \in \{-2, 0, 2\}$. The result is a generated output voltage with 9 levels: $u_s \in \{4, 3, 2, 1, 0, 1, 2, 3, 4\}$. Some levels of the output voltage can be generated by different commutation sequences. For example, there are four possible commutation sequences resulting in $u_s = 2\,p.u.$, $(u_{p1}, u_{p2}, u_{p3}) \in \{(1, 1, 2); (0, 0, 2); (1, 1, 2); (1, 1, 0)\}$. The dashed lines in Fig. 3 show the commutation sequence $(u_{p1}, u_{p2}, u_{p3}) = (1, 1, 0)$. These redundant combinations can be selected in order to optimize the switching process of the inverter [11].

These different possibilities offered by the output voltage of the partial inverters, and the redundancies among them to deliver a same output voltage level, can be considered as degrees of freedom which can be exploited in order to optimize the use of a AMI.

III. MULTILEVEL INVERTERS CONTROL STRATEGIES

Several modulation strategies have been proposed for

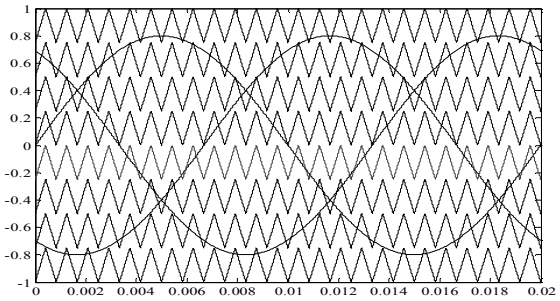

Fig. 4. Multi-carrier PWM generation for $N = 9$ levels (with $m = 24$ and $r = 0.8$).

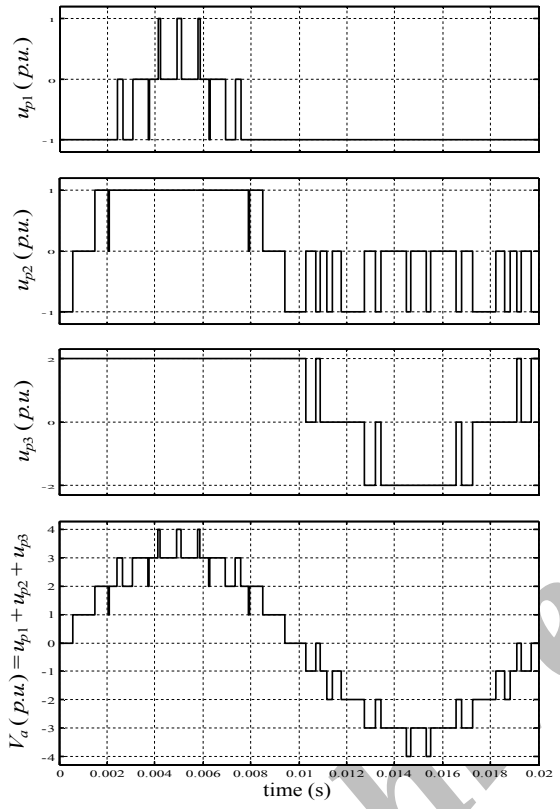

Fig. 5. Output voltages of each partial inverter and total output voltage V_a of the 9-level USAMI controlled by the MCPWM (with $m = 24$ and $r = 0.8$).

symmetrical multilevel converters. They are generally derived from the classical modulation techniques used for more traditional converters [11]. Among these methods, the most common used is the multi-carrier sub-harmonic PWM technique. This modulation method can also be used to control asymmetrical multilevel power converters. In the case of AMIs, other kinds of modulation can be used [4].

In this Section, we briefly introduce the MCPWM technique. We also propose a HES based on ANNs. These control strategies will be compared by computer simulations. The objective is to elaborate optimized switching angles for an 9-level USAMI. The inverter is then employed to supply an asynchronous machine.

A. Multi-Carrier PWM (MCPWM)

The principle of the MCPWM is based on a comparison of a sinusoidal reference waveform with vertically shifted carrier waveforms. N-1 carriers are required to generate N levels. As shown in Fig. 4, the carriers are in continuous bands around the reference zero. They have the same amplitude A_c and the same frequency f_c. The sine

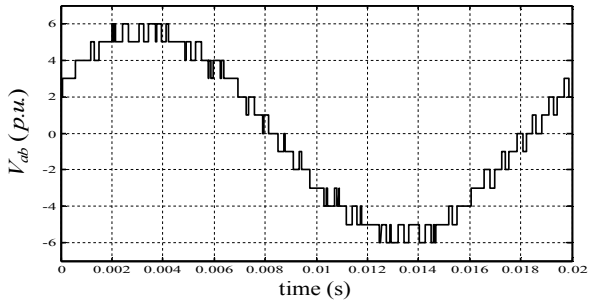

Fig. 6. Output voltage V_{ab} of the 9-level USAMI controlled by the MCPWM (with $m = 24$ and $r = 0.8$).

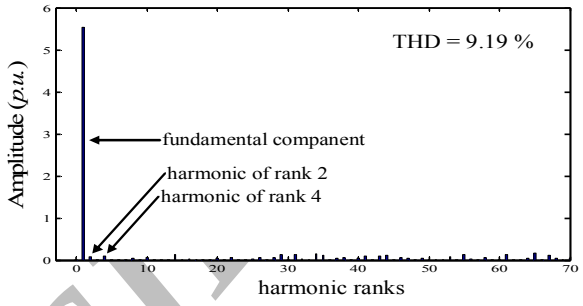

Fig. 7. Frequency content of the output voltage V_{ab} with the MCPWM strategy (with $m = 24$ and $r = 0.8$).)

reference waveform has a frequency f_r and an amplitude A_r. At each instant, the result of the comparison is 1 if the triangular carrier is greater than the reference signal and 0 otherwise. The output of the modulator is the sum of the different comparisons which represents the voltage level. The strategy is therefore characterized by the two following parameters [7], respectively called the modulation index and the modulation rate

$$m = \frac{f_c}{f_r} \tag{5}$$

$$r = \frac{2}{N-1}\frac{A_r}{A_c} \tag{6}$$

We propose to develop a 9-level inverter composed of $k = 3$ partial inverters per phase with the following dc-voltage sources: $u_{d1} = 1$ *p.u.*, $u_{d2} = 1$*p.u.* and $u_{d3} = 2$ *p.u.* The output voltages u_{p1}, u_{p2} and u_{p3} of each partial inverter and the resulting voltage for the first phase are represented by Fig. 5. The output voltage V_{ab} and its frequency representation are respectively presented by Fig. 6 and Fig. 7.

B. Harmonics Elimination Strategy with ANNs

1) Harmonics Elimination Strategy (HES)

The HES is based on the Fourier analysis of the generated voltage u_s at the output of the USAMI (see Fig. 2) [13]. This voltage is symmetric in a half and a quarter of a period. As a result, the even harmonic components are null. The Fourier series expansion for the u_s voltage is thus

$$\begin{cases} u_s = \sum_{n=1}^{\infty} u_n \sin n\omega t \\ u_n = \dfrac{4u_{d1}}{n\pi}\sum_{i=1}^{p} \cos n\theta_i \end{cases} \tag{7}$$

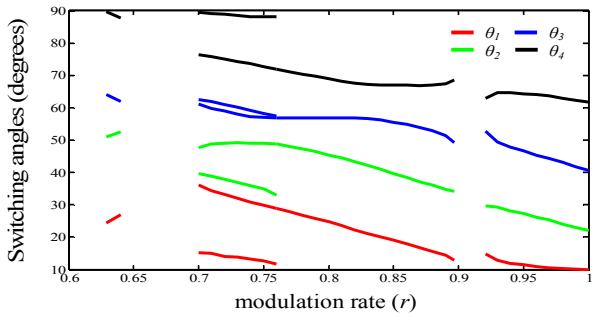

Fig. 8. All switching angles versus r.

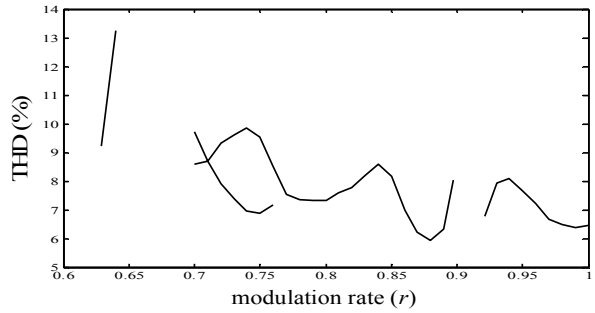

Fig. 9. THD versus r for all switching angles.

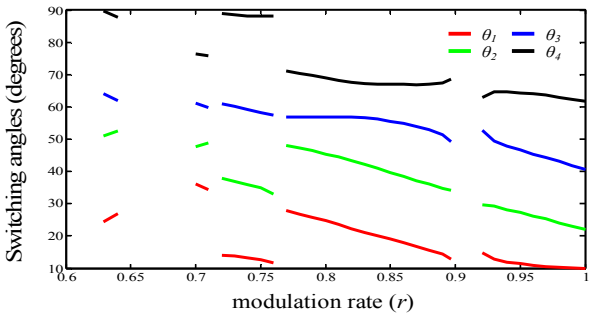

Fig. 10. Switching angles versus r leading to the lowest THD.

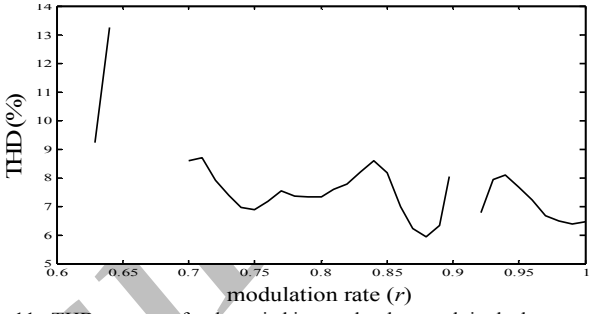

Fig. 11. THD versus r for the switching angles that result in the lowest total harmonic distortion.

where u_n represents the amplitude of the harmonic term of rank n, $p=(N\text{-}1)/2$ is the number of switching over a quarter of a period, and θ_i are the switching angles ($i=1,\ 2...,p$).

The p switching angles in (7) are calculated by fixing the amplitude of the fundamental term and by canceling the $p-1$ other harmonic terms. Practically, four switching angles $(\theta_1,\theta_2,...\ \theta_4)$ are necessary for canceling the three first harmonics terms (i.e., harmonics with a odd rank and non multiple of 3, therefore 5, 7 and 11) in the case of a three phase 9-level USAMI composed of $k=3$ partial inverters per phase supplied by the dc-voltages $u_{d1}=1\ p.u.$, $u_{d2}=1 p.u.$ and $u_{d3}=2\ p.u.$ These switching angles can be determined by solving the following system of non linear equations

$$\begin{cases} \sum_{i=1}^{4}\cos\theta_i=\pi r \\ \sum_{i=1}^{4}\cos n\theta_i=0 \quad \text{for } n\in\{5,\ 7,\ 11\} \end{cases} \tag{8}$$

where $r=u1/4u_{d1}$ is the modulation rate. The solution of (8) must also satisfy

$$\theta_1<\theta_2<\theta_3<\theta_4<\frac{\pi}{2} \tag{9}$$

and can be solved by applying the Newton-Raphson method. This method returns all the possible combinations of the switching angles for different values of *r*. The result is represented by Fig. 8 where one can see the presence of two possible solutions of angles for $0.70 \le r \le 0.76$. On the other side, the system does not accept any solution for $r<0.629$, $0.64<r<0.7$ and $0.897<r<0.921$. The system has an unique solution for all the other values of r.

In the case of two possible solutions for an angle θ_1, the criteria for selecting one of them can be the Total Harmonic Distortion (THD). The best angle values are therefore the ones leading to the lowest THD. The THD is a quantifiable expression for determining how much the signal has been distorted. The greater are the amplitudes of the harmonics, the greater are the distortions. The THD is defined by

$$THD=\sqrt{\sum_{n=2}^{\infty}\left(\frac{1}{n}\sum_{i=1}^{p=4}\cos n\theta_i\right)^2}\Bigg/\sum_{i=1}^{p=4}\cos\theta_i \tag{10}$$

This is shown in Fig. 9 corresponding to the solutions given in Fig. 8. Choosing the switching angles based on this criteria, the multiple switching angle solutions given in Fig. 8 reduce to the single set of solutions given in Fig. 10, and the corresponding THD is shown in Fig. 11.

The control of an AMI with the HES in a real-time application requires to memorize all the switching angles. A considerable computational memory space must therefore be involved for the implementation of this control law.

2) Application of ANNs

ANNs have gained increasing popularity and have demonstrated superior results compared to alternative methods in many studies. Indeed, ANNs are able to map underlying relationship between input and output data without prior understanding of the process under investigation. This mapping is achieved by adjusting their internal parameters called weights from data. This process is called the learning or the training process. Their interest comes also from their generalization capabilities, i.e., their ability to deliver estimated responses to inputs that were not seen during training. Hence, the application of ANNs to complex relationships and processes makes them highly attractive for different types of modern problems [9]-[14].

We use a neural network to learn the switching angles previously provided by the Newton-Raphson method. The approach aims to replace the painful memorization of the angles in order to make its implementation realizable in a real-time application. MLPs [10] are well suited for this task. Associated to the backpropagation learning rule, they are known as universal approximators [9].

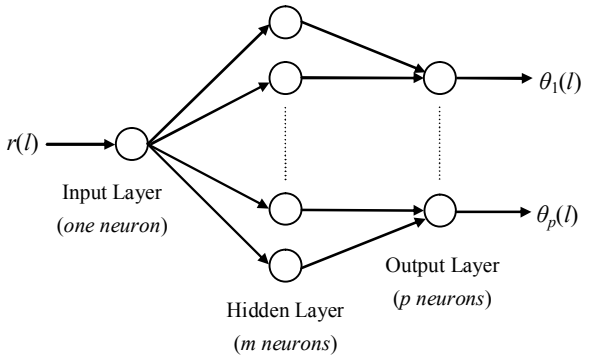

Fig. 12. Multi-Layer Perceptron network topology ($1\times m\times p$) used to generate switching angles.

An MLP network is composed of a number of identical units called neurons organized in layers, with those on one layer connected to those on the next layer (except for the last layer or output layer). Indeed, MLPs architecture is structured into an input layer of neurons, one or more hidden layers and one output layer. Neurons belonging to adjacent layers are usually fully connected and the activation function of the neurons is generally sigmoidal or linear. In fact, the various types and architectures are identified both by the different topologies adopted for the connections and by the choice of the activation function.

Some parameters of ANNs can not be determined from an analytical analysis of the process under investigation. This is the case of the number of hidden layers and the number of neurons belonging to them. Consequently, they have to be determined experimentally according to the precision which is desired for the estimation. The number of inputs and outputs depends from the considered process. In our application, the MLP has to map the underlying relationship between the modulation rate (input) and the p witching angles (output). The MLP shown in Fig. 12 is composed by one input neuron and p output neurons.

The MLP must be trained in order to adjust and to find the adequate weights. This is achieved by using probabilistic learning techniques and with data from the process under investigation. The training data consists of the inputs R and the corresponding desired output vectors S:

$$R=\left[r(1)\ \ldots\ r(l)\ \ldots\ r(n)\right] \tag{11}$$

$$S=\left[S(1)...S(l)...S(n)\right]=\begin{bmatrix}\theta_1(1) & \cdots & \theta_1(l) & \cdots & \theta_1(n)\\ \vdots & & \vdots & & \vdots\\ \theta_p(1) & \cdots & \theta_p(l) & \cdots & \theta_p(n)\end{bmatrix} \tag{12}$$

In the last two expressions, $l=1....n$, where n is the number of examples. For a given input $r(l)$, the MLP computes an estimated output vector $\hat{S}(l)=[\hat{\theta}_1(l)\ldots\hat{\theta}_p(l)]$ that must be as close as possible to the ideal desired output $S(l)$. The difference $E(l)=(\hat{S}(l)\text{-}S(l))^2$ constitutes the squared output error for example l that is used by the training algorithm to correct the weights of the neurons. This is repeated for the n samples composing the training data set until convergence is reached. The learning is achieved with the backpropagation algorithm [9].

After the training process, the MLP is able to estimate the angles corresponding to an input $r(l)$. In other words, the MLP has learned the functions $\theta_i=f_i(r)$ with $f_i(r)$ are functions tabulated value ($i=1...4$). By approximating these functions, the MLP will be able to deliver the angles for the real-time control of the inverter.

TABLE I
APPROXIMATION FUNCTIONS WITH VARIOUS SIZES OF THE MLP

MLP architecture	Required iterations	Learning error (degrees)
1×2×4	10000	4.372
1×4×4	10000	3.213
1×6×4	10000	2.105
1×7×4	10000	1.467
1×8×4	8943	0.893
1×9×4	6671	0.677
1×10×4	4249	8×10^{-2}
1×11×4	2637	4×10^{-3}
1×12×4	1528	1×10^{-3}

IV. RESULTS

A. Learning Performance

The MLP is applied for canceling harmonics 5, 7 and 11 at the output of the USAMI. The training set is elaborated from the Newton-Raphson method and the optimal angles are the ones resulting in the lowest THD when several solutions exist.

An MLP with one hidden layer is used with a training set of $n=33$ examples. Several tests have been conducted for determining the number of neurons of the hidden layer. Results are provided by Table I. These tests have been achieved because there are no generally acceptable theories, solutions being in the specific literature only for special cases. The determination of number of neurons in hidden layers is very important as it affects the training time and generalization property of neural networks.
According to the results given by Table I, a MLP with 12 neurons in the hidden layer has been adopted. The approximating function remains the same with 12 neurons as with a higher number of neurons in the hidden layer. This configuration has been chosen after different experiments, it represents the best compromise between computational costs and performances. The other parameters of the MLP are detailed in Table II.

The learning convergence of the 1×12×4-MLP is reached after 1528 epochs, and leads to angle errors less than 0.001 degrees. Since the error is very small, the outputs delivered by the MLP are therefore very close to the angles given by the Newton-Raphson method. The estimated angles are represented by Fig. 13. The evolution of the training Sum-Squared-Error (SSE) is shown by Fig. 14.

After learning, the MLP is also able to deliver the angles for inputs which were not present in the training set. Theses generalization capabilities are very interesting in our application, the neural controller is therefore always able to deliver the control signals for the inverter. For example, Fig. 15 to 17 shows the results obtained for an input which was not in the training set, $r(l)=0.8$ which theoretically corresponds to $\theta_1=24.6999^o$, $\theta 2$=45.5307°, θ_3=57.0398° and $\theta 4=68.8887^o$.

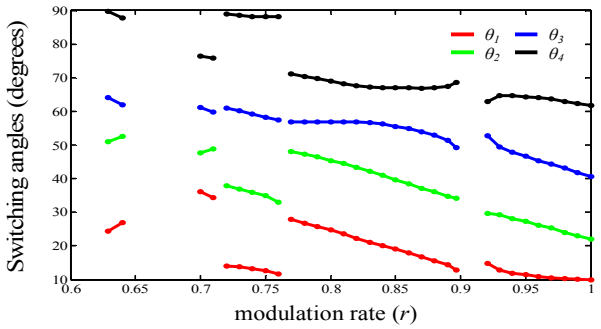

Fig. 13. Switching angles versus r learned by the MLP (•), and calculated with Newton-Raphson method (–).

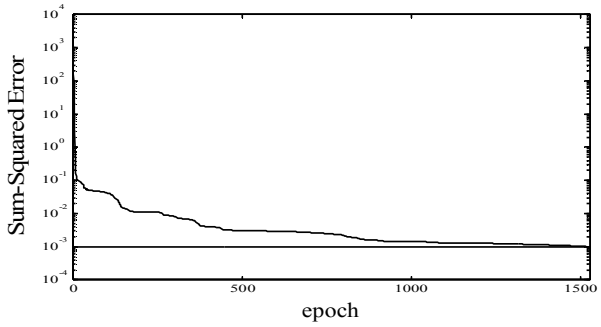

Fig. 14. Training error.

TABLE II
PROPERTIES OF THE MLP

MLP parameters	values
Network configuration	1×12×4
Transfer functions	tansig, purelin
Training technique	Levenberg-Marquardt
Learning rate	0.1
Momentum constant	0.9
Training goal	0.001
Training examples	33
Epochs	1528
Maximum epochs	10 000

B. Performance in Supplying an Asynchronous Machine

In order to evaluate the performance and the robustness of the proposed approach, a 9-level USAMI is used to supply an asynchronous machine with open-loop control. The closed-loop control with other approaches, such as space vector modulation (SVM) is presented in [15]. The neural HES is compared to the MCPWM strategy in controlling the 9-level USAMI. The objective is to use the proposed neural strategy in order to minimize the harmonics absorbed by the asynchronous machine.

The results of the control based on the MCPWM are presented by Fig. 18 and Fig. 19. This first figure shows the stator current and the electromagnetic torque with significant fluctuations. The second figure shows the frequency content of the stator current. Results by using neural approach with the MLP issued for the previous learning process are presented by Fig. 20 and Fig. 21. By comparing Fig. 19 to Fig. 21, it can be deduced that the neural HES efficiently cancels the harmonics of ranks 5, 7, and 11 from the output voltage V_{ab}. Moreover, the

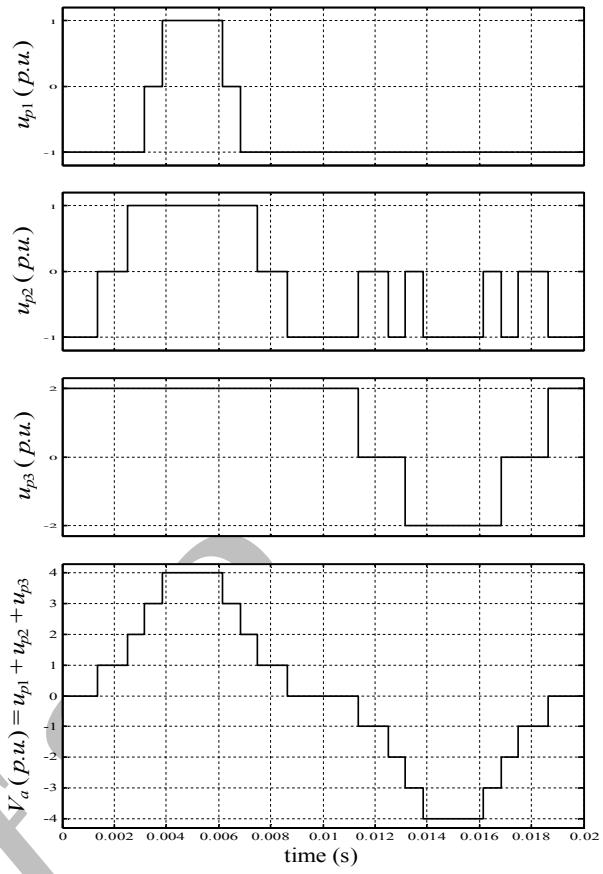

Fig. 15. Output voltages of each partial inverter and total output voltage V_a of the 9-level USAMI controlled by the proposed neural HES (with $r(l) = 0.8$ and $p = 4$).

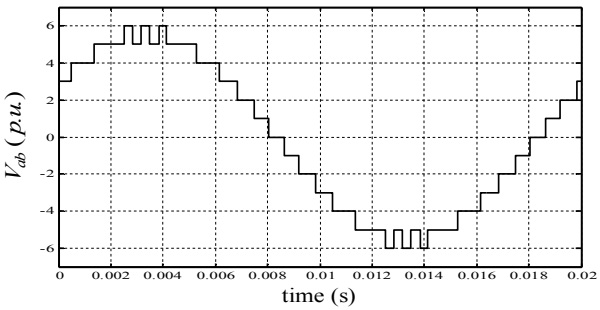

Fig. 16. Output voltage V_{ab} of the 9-level USAMI controlled by the proposed neural HES (with $r(l) = 0.8$ and $p = 4$).

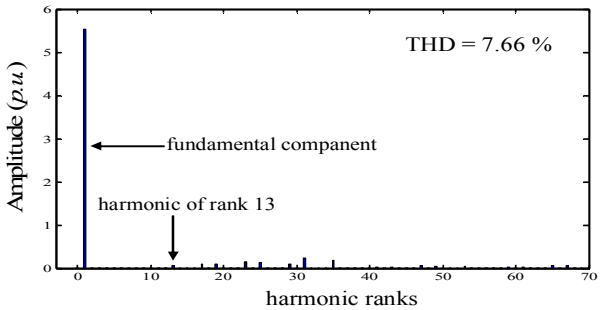

Fig. 17. Frequency content of the output voltage V_{ab} with the proposed neural HES (with $r(l) = 0.8$ and $p = 4$).

amplitudes of the harmonic distortions are very small compared to the amplitude of the fundamental component.

Performances obtained with both methods are summarized in Table III. The THD measured on V_{ab} and resulting from the neural approach of the HES is smaller than the one obtained with the MCPWM method. The THD

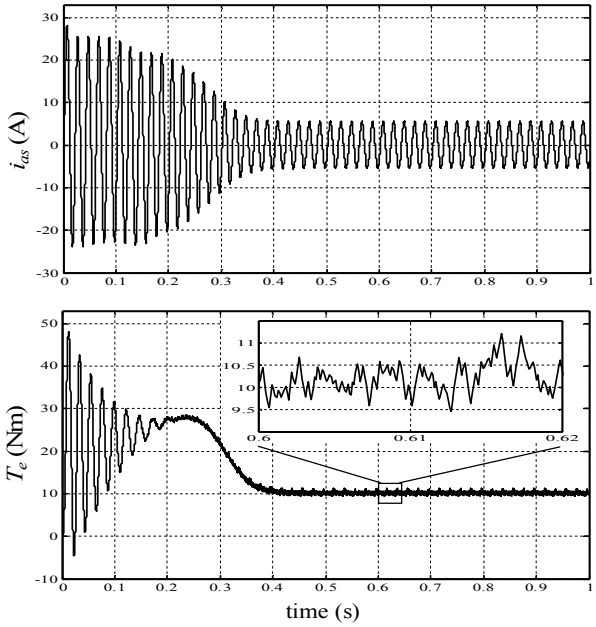

Fig. 18. Stator current (top) and electromagnetic torque (bottom) of the asynchronous machine fed by a 9-level USAMI controlled by the MCPWM.

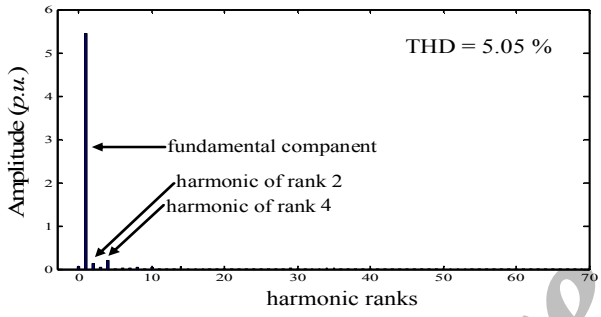

Fig. 19. Frequency content of the stator current of the asynchronous machine fed by a 9-level USAMI controlled by the MCPWM.

TABLE III
PERFORMANCES OF THE CONTROL METHODS

Control method	V_{ab} THD (%)	i_{as} THD (%)	f_{Cem} (Hz)	Δ_{Cem} (Nm)	N_b of θ_i
MCPWM	9.19	5.05	f	1.77	$2m = 48$
Neural HES	7.66	1.92	$2f$	1.31	4p=16

measured on the stator current i_{as} is reduced by a factor 2.63 with the neural HES compared to the MCPWM method. The control is thus optimized with the neural HES in order to avoid the asynchronous machine to absorb harmonics.

It can also be seen that the electromagnetic torque continuously oscillates at a frequency f with the MCPWM method (because of the harmonics of rank 2 and 4 which are present in the output voltage). The torque oscillates at $2f$ with the neural approach. The neural method also reduced the number of switching angles by a factor 3 compared to the MCPWM method which is highly appreciated for the electronic devices.

V. CONCLUSIONS

The control strategy of an inverter used to feed an asynchronous machine is crucial and determines the performances of the motor task. In this study, we propose a low-cost neural implementation of a HES to control a uniform step asymmetrical 9-level inverter. A theoretical analysis of the proposed solving algorithm with neural networks is provided. The neural implementation of the HES uses very few computational costs and is therefore well suited for real-time applications. This neural approach is compared to the MCPWM strategy. Simulation results are given to show the high performance and technical advantages of the neural implementation of the HES for the control of a uniform step asymmetrical 9-level inverter. In the motor supply application, the neural method efficiently cancels the harmonic distortions and ensures a high quality torque. Moreover, the neural controller allows reducing the switching losses and prolonging the life cycle of the electronic devices.

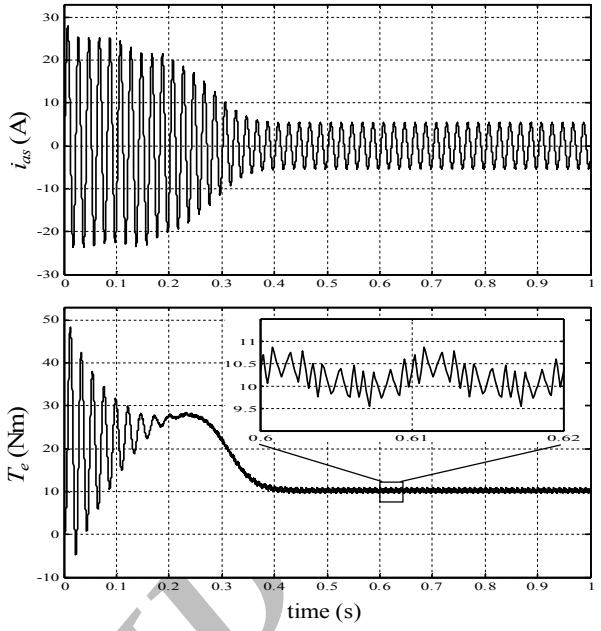

Fig. 20. Stator current (top) and electromagnetic torque (bottom) of the asynchronous machine fed by a 9-level USAMI controlled by the proposed neural HES.

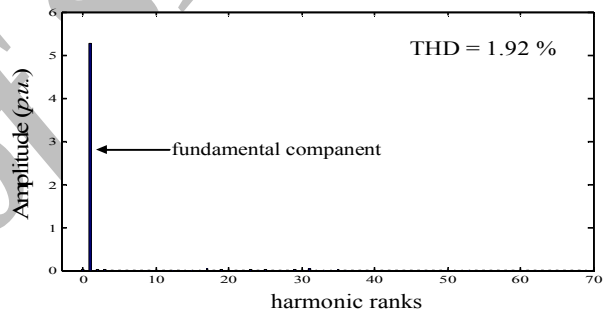

Fig. 21. Frequency content of the stator current of the asynchronous machine fed by a 9-level USAMI controlled by the proposed neural HES.

APPENDIX

Supply voltages of the partial inverters with:
PU Units:
$u_{d1} = 1$, $u_{d2} = 1$ and $u_{d3} = 2$.
SI Units:
$U_{d1} = 100$ V, $U_{d2} = 100$ V and $U_{d3} = 200$ V.
Asynchronous machine data:
Stator resistance $R_s = 4.850\,\Omega$, Rotor resistance $R_r = 3.805\,\Omega$, Stator inductance $L_s = 0.274$ H, Rotor

inductance $L_r = 0.274\,\text{H}$, Mutual inductance $L_m = 0.258\,\text{H}$, Number of pole pairs $P = 2$, Rotor inertia $J = 0.031\ \text{kg.m}^2$, Viscous friction coefficient $K_f = 0.00136\ \text{Nm.s.rad}^{-1}$.

REFERENCES

[1] J. Rodriguez, J. S. Lai, and F. Z. Peng, "Multilevel inverters: a survey of topologies, controls, and applications," *IEEE Trans. on Industrial Electronics*, vol. 49, no. 4, pp. 724-738, Aug. 2002.

[2] M. D. Manjrekar, *Topologies, Analysis, Controls and Generalization in H-Bridge Multilevel Power Conversion*, Ph.D. Thesis, University of Wisconsin, Madison, 1999.

[3] L. Delmas, T. Meynard, H. Foch, and G. Gateau, "SMC: stacked multicell converter," in Proc. *PCIM 2001*, vol. 43, pp. 63-69, 2001.

[4] S. Mariethoz, *Etude Formelle Pour La Synthèse De Convertisseurs Multiniveaux Asymétriques: Topologies, Modulation Et Commande (in French)*, Ph.D. Thesis, EPF-Lausanne, Switzerland, 2005.

[5] D. O. Abdeslam, P. Wira, J. Merckl, D. Flieller, and Y. A. Chapuis, "A Unified artificial neural network architecture for active power filters," *IEEE Trans. on Industrial Electronics*, vol. 54, no. 1, pp. 61-76, Feb. 2007.

[6] B. P. McGrath and D. G. Holmes, "Multicarrier PWM Strategies for Multilevel Inverters," *IEEE Trans. on Industrial Electronics*, vol. 49, no. 4, pp. 858-867, Aug. 2002.

[7] J. Song-Manguelle, S. Mariethoz, M. Veenstra, and A. Rufer, "A Generalized design principle of a uniform step asymmetrical multilevel converter for high power conversion," in *Proc. European Conf. on Power Electronics and Applications, EPE'01*, Graz, pp. 1-12, Austria, Aug. 2001.

[8] J. N. Chiasson, L. M. Tolbert, K. J. McKenzie, and Z. Du, "A unified approach to solving the harmonic elimination equations in multilevel converters," *IEEE Trans. on Power Electronics*, vol. 19, no. 2, pp. 478-490, Mar. 2004.

[9] S. Haykin, *Neural Networks: A Comprehensive Foundation*, Prentice Hall, Upper Saddle River, N.J., 2nd edition, 1999.

[10] C. M. Bishop, *Neural Networks for Pattern Recognition*, Clarendon Press, Oxford, 1995.

[11] J. Song-Manguelle, *Convertisseurs Multiniveaux Asymétriques Alimentés par Transformateurs Multi-Secondaires Basse-Fréquence: Réactions Au Réseau D'alimentation,* (in french), Ph.D. Thesis, EPF-Lausanne, Switzerland, 2004.

[12] S. Mariéthoz and M. Veenstra, "Alimentation d'onduleurs multiniveaux asymétriques: analyse des possibilités de réalisation et méthodes de répartition de la puissance (in french)," *Revue internationale de génie électrique (RIGE)*, vol. 7, no. 3-4, pp. 263-278, Jun. 2004.

[13] M. S. A. Dahidah and V. G. Agelidis, "Selective harmonic elimination PWM control for cascaded multilevel voltage source converters: a generalized formula," *IEEE Trans. on Power Electronics*, vol. 23, no. 4, pp. 1620-1630, Jul. 2008.

[14] S. Khomfoi and L. M. Tolbert, "Fault diagnostic system for a multilevel inverter using a neural network," *IEEE Trans. on Power Electronics*, vol. 22, no. 3, pp. 1062-1069, May 2007.

[15] T. Bessaad, *Commande Par Modulation Vectorielle (SVM) D'un Onduleur Multiniveau Asymétrique à pas Uniforme (in french)*, M.S. thesis, Univ. Chlef, Algeria, 2009.

R. Taleb was born in Chlef, Algeria, in 1974. He received the B.S. and M.S. degrees in electrical engineering from the University of Hassiba Ben Bouali, Chlef, Algeria, in 1999 and 2004, respectively. He is currently working towards the Ph.D. degree at the University of Sidi Bel-Abbes, Algeria. He joined the Department of Electrical Engineering from the University of Chlef, Algeria, in 2004, where he is actually a Research Assistant.

His research interest includes artificial neural networks, genetic algorithms, fuzzy logic, multilevel inverters and motor drives.

A. Meroufel was born in Sidi Bel-Abbes, Algeria, in 1954. He received the B.S. and M.S. degrees in electrical engineering from the Université des Sciences et de la Technologie, Oran, Algeria, in 1979 and 1990 respectively, and the Ph.D. degree in electrical engineering from the Electrical Engineering Institute of the University of Sidi Bel-Abbes, Algeria, in 2004. He is currently an Associate Professor of electrical engineering in this University since 1986.

He is a team leader in the ICEPS (Intelligent Control Electrical Power System) Laboratory. His research interest includes artificial neural networks, fuzzy logic and applications to power electronics, PWM techniques, drives, and electric machine control.